


Combination of sacubitril/valsartan and blockade of the PI3K pathway enhanced kidney protection in a mouse model of cardiorenal syndrome

Shunichiro Tsukamoto¹, Hiromichi Wakui^{1,*}, Tatsuki Uehara¹, Yuka Shiba¹, Kengo Azushima¹, Eriko Abe¹, Shohei Tanaka¹, Shinya Taguchi¹, Keigo Hirota¹, Shingo Urate¹, Toru Suzuki¹, Takayuki Yamada^{1,2}, Sho Kinguchi¹, Akio Yamashita³, and Kouichi Tamura ^{1,*}

¹Department of Medical Science and Cardiorenal Medicine, Yokohama City University Graduate School of Medicine, 3-9 Fukuura, Kanazawa-ku, 236-0004 Yokohama, Japan; ²Renal-Electrolyte Division, Department of Medicine, University of Pittsburgh, Pittsburgh, PA, USA; and ³Department of Investigative Medicine Graduate School of Medicine, University of the Ryukyus, Okinawa, Japan

Received 9 June 2023; revised 21 September 2023; accepted 25 September 2023; online publish-ahead-of-print 29 September 2023

Handling Editor: Daniel FJ Ketelhuth

Aims

Angiotensin receptor-neprilysin inhibitor (ARNI) is an established treatment for heart failure. However, whether ARNI has renoprotective effects beyond renin-angiotensin system inhibitors alone in cardiorenal syndrome (CRS) has not been fully elucidated. Here, we examined the effects of ARNI on the heart and kidneys of CRS model mice with overt albuminuria and identified the mechanisms underlying ARNI-induced kidney protection.

Methods and results

C57BL6 mice were subjected to chronic angiotensin II infusion, nephrectomy, and salt loading (ANS); they developed CRS phenotypes and were divided into the vehicle treatment (ANS-vehicle), sacubitril/valsartan treatment (ANS-ARNI), and two different doses of valsartan treatment (ANS-VAL M, ANS-VAL H) groups. Four weeks after treatment, the hearts and kidneys of each group were evaluated. The ANS-vehicle group showed cardiac fibrosis, cardiac dysfunction, overt albuminuria, and kidney fibrosis. The ANS-ARNI group showed a reduction in cardiac fibrosis and cardiac dysfunction compared with the valsartan treatment groups. However, regarding the renoprotective effects characterized by albuminuria and fibrosis, ARNI was less effective than valsartan. Kidney transcriptomic analysis showed that the ANS-ARNI group exhibited a significant enhancement in the phosphoinositide 3-kinase (PI3K)-AKT signalling pathway compared with the ANS-VAL M group. Adding PI3K inhibitor treatment to ARNI ameliorated kidney injury to levels comparable with those of ANS-VAL M while preserving the superior cardioprotective effect of ARNI.

Conclusion

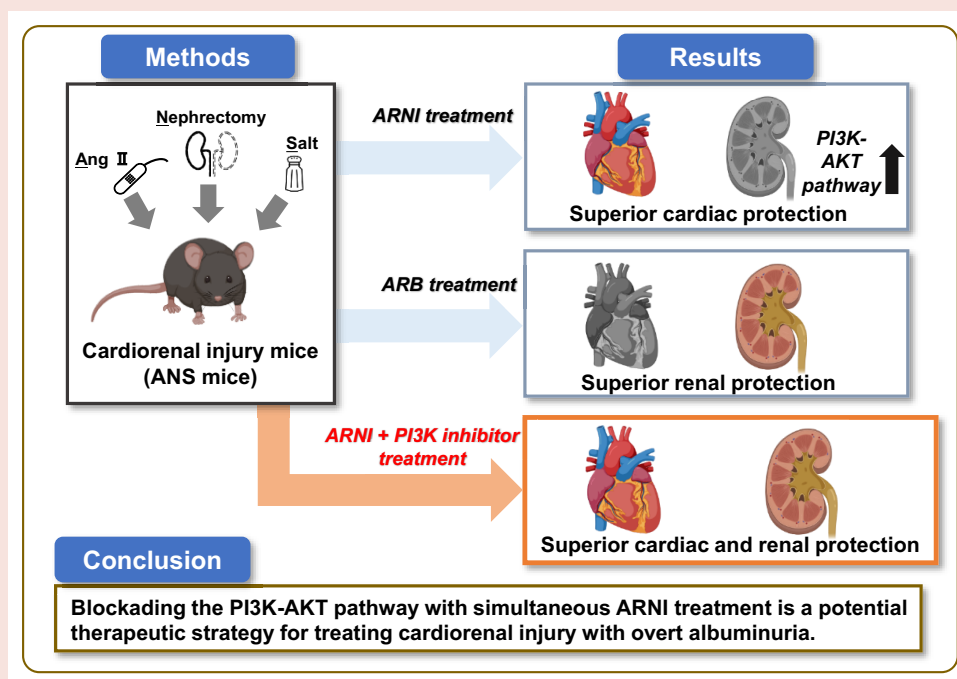
PI3K pathway activation has been identified as a key mechanism affecting remnant kidney injury under ARNI treatment in CRS pathology, and blocking the PI3K pathway with simultaneous ARNI treatment is a potential therapeutic strategy for treating CRS with overt albuminuria.

* Corresponding authors. Tel: 81 45 787 2635, Fax: 81 45 701 3738, Email: hiro1234@yokohama-cu.ac.jp (H.W.); Email: tamukou@yokohama-cu.ac.jp (K.T.)

© The Author(s) 2023. Published by Oxford University Press on behalf of the European Society of Cardiology.

This is an Open Access article distributed under the terms of the Creative Commons Attribution-NonCommercial License (<https://creativecommons.org/licenses/by-nc/4.0/>), which permits non-commercial re-use, distribution, and reproduction in any medium, provided the original work is properly cited. For commercial re-use, please contact journals.permissions@oup.com

Graphical Abstract



Keywords

Angiotensin receptor-neprilysin inhibitor • Angiotensin II receptor blocker • Cardiorenal injury • Albuminuria • Phosphoinositide 3-kinase inhibitor • Heart failure

Translational perspective

This study demonstrated the robustness of the cardioprotective effect of ARNI. However, ARB alone may be superior in protecting the kidneys in hyperfiltration conditions with overt albuminuria. One of the mechanisms involved in establishing phenotypic differences in kidneys between ARNI and ARB alone may be the enhancement of the PI3K-AKT pathway. PI3K pathway activation has been identified as a key mechanism for remnant kidney injury under ARNI treatment in cardiorenal syndrome model mice, and simultaneous blockade of the PI3K pathway with ARNI may be a therapeutic strategy to treat cardiorenal syndrome with overt albuminuria.

Introduction

Treatments for organ injury and failure have typically focused on a single organ. However, the importance of linkages between organs has been highlighted in recent years, and novel treatment strategies are increasingly being developed to target multiple organs. Notably, the heart and kidneys are closely related and interdependent.^{1,2} The frequency of chronic kidney disease and heart failure (HF) is increasing, and in many cases, patients have both diseases.^{3,4} Therefore, the development of effective treatments for patients with both diseases is urgently needed.

Angiotensin receptor-neprilysin inhibitor (ARNI), a combination of neprilysin inhibitor (NEP-I) and angiotensin II (Ang II) receptor blocker (ARB), is an established treatment for patients with HF. NEP-I inhibits the degradation of natriuretic peptides (NPs) and thereby enhances their effects, which include promoting myocardial relaxation and reducing hypertrophy through a cyclic guanosine monophosphate-dependent pathway.⁵⁻⁷ Additionally, ARNI prevents myocardial fibrosis⁸⁻¹² and inflammatory^{13,14} by inhibiting several pathways, such as the transforming

growth factor-beta (TGF- β)/Smad pathway or Wnt/ β -catenin pathway.⁶⁻¹⁴ In several randomized controlled trials, administration of sacubitril/valsartan, first-in-class ARNIs, reduced hospitalizations for HF and cardiovascular death in patients with HF compared with renin-angiotensin system (RAS) inhibitors alone.^{15,16} Based on these results, ARNI has been recommended for patients with HF.^{17,18}

The effect of ARNI on kidneys has also attracted attention. In PARADIGM-HF and PARAGON-HF trials, sacubitril/valsartan treatment reduced renal events and the decline in the estimated glomerular filtration rate (eGFR) in patients with HF compared with RAS inhibitors.^{15,16,19,20} These findings suggest that ARNI treatment exerts renoprotective effects in addition to cardioprotection in HF patients. Natriuretic peptides, enhanced by ARNI, promote natriuresis and increase intraglomerular pressure and GFR through increased kidney perfusion and predominant dilation of afferent arteries.^{21,22} These effects likely protected the kidneys under reduced perfusion due to an acute decrease in cardiac output. In cardiorenal syndrome (CRS) with overt albuminuria, however, it is unclear whether these effects

of ARNIs are more beneficial to the kidneys than RAS inhibitors that can reduce intraglomerular pressure.²³ In the PARADIGM-HF study, sacubitril/valsartan treatment was associated with higher albuminuria compared with valsartan alone.¹⁹ In the United Kingdom Heart and Renal Protection-III (UK HARP-III) trial in patients with increased albuminuria and advanced kidney impairment, sacubitril/valsartan treatment was not found to effectively preserve eGFR compared with irbesartan.²⁴ Consequently, whether ARNIs provide better kidney protection than ARBs, especially under conditions of chronic glomerular hyperfiltration and high albuminuria, remains controversial. Furthermore, to the best of our knowledge, no basic experiments have been conducted to evaluate the effects of ARNI on the kidneys under such conditions.

To address this lack of data, in the present study, we investigated the effects of ARNI on the heart and kidneys using a mouse model of CRS with overt albuminuria. Cardiorenal syndrome model mice were treated with chronic Ang II infusion, nephrectomy, and salt loading (mice with ANS).²⁵ Additionally, we explored the mechanisms underlying the differential effects of ARNI and valsartan on kidneys and investigated the possible protective mechanism of ARNI in a CRS mouse model.

Methods

Animal experiments

This study was performed in accordance with the National Institutes of Health guidelines for the use of experimental animals. All animal studies were reviewed and approved by the Animal Studies Committee of Yokohama City University. The mice were housed in a controlled environment with a 12-h light–dark cycle (lights on 7 a.m. to 7 p.m. local time) at a temperature of 25°C. The mice were allowed free access to food and water.

Mice with ANS and treatment

Experiments were performed using 9–10-week-old male C57BL/6J mice [purchased from the Charles River Laboratories (Wilmington, MA, USA)] after 1-week of acclimatization in all groups (each group, $n = 6$). All mice were fed a standard diet (0.5% NaCl, 3.6 kcal/g, and 13.3% energy as fat; Oriental MF; Oriental Yeast Co., Ltd). After anaesthesia with isoflurane (2%), the abdomen of the mice was incised and the left kidney was removed. Mice in the control group underwent a sham operation in which the left kidney was exposed without removal. To perform Ang II infusion, Ang II (1.2 mg/kg/day) was infused subcutaneously in mice for 4 weeks using an osmotic minipump (model 1004; ALZET) after nephrectomy. The mice were further divided into the following four groups: vehicle treatment (ANS-vehicle group), sacubitril/valsartan treatment [60 mg/kg/day (sacubitril 30 mg/kg/day, valsartan 30 mg/kg/day), orally administered (ANS-ARNI group)], moderate-dose valsartan treatment [30 mg/kg/day, orally administered (ANS-VAL M group)], and high-dose valsartan [60 mg/kg/day orally administered (ANS-VAL H group)]. The mice were provided drinking water containing 0.9% NaCl (Otsuka Pharmaceutical, Tokyo, Japan). The mice in the control group received saline subcutaneously via an osmotic pump and were provided with water without NaCl.

For phosphoinositide 3-kinase (PI3K) inhibitor treatment, the ANS-ARNI and ANS-VAL M groups received Ly294002 (Selleck Chemicals) at a dose of 30 mg/kg intraperitoneally three times per week for 4 weeks after the operation.

Blood pressure and heart rate measurements

Systolic blood pressure (BP) and heart rate (HR) were measured using the tail-cuff method (BP-Monitor MK-2000; Muromachi Kikai Co., Tokyo, Japan), as described previously.²⁶ All measurements were performed between 9 a.m. and 2 p.m. At least 10 measurements were performed for each mouse, and the mean value was used for analysis.

Echocardiography

The mice were anaesthetized with isoflurane (2%) and fixed on an echo pad in the supine position. Echocardiography was performed using a

Vevo3100LT imaging system (FUJIFILM VisualSonics Inc.) before the operation and at 2 and 4 weeks after the operation. Short-axis M-mode images were recorded at the papillary muscle level. After measurement, software analysis was performed to calculate the left ventricular inner diameter contraction ratio (left ventricular fractional shortening, LVFS). Calculations were performed at three different points for each measurement.

Biochemical analysis

Metabolic cage analysis was performed at 2 and 4 weeks after the operation, as described previously.^{26,27} The mice were housed in metabolic cages for 2 consecutive days and provided free access to food and water. A 24 h urine collection procedure was performed on Day 2. At 4 weeks after surgery, blood samples were collected by cardiac puncture in the fed state after inhalation of 5% isoflurane anaesthesia. The mice were killed humanely after anaesthesia, as described previously.²⁶ Whole blood samples were centrifuged at 650 g. (MR-150; Tomy Seiko Co., Ltd, Tokyo, Japan) at 4°C for 10 min to separate the plasma. The resulting plasma samples were stored at –80°C until use. Plasma creatinine, urinary creatinine, and urinary albumin concentrations were measured using a Hitachi 7180 autoanalyser (Hitachi, Tokyo, Japan).

Histological analyses

Histological analyses were performed as described previously.²⁸ Briefly, mouse heart and kidneys were fixed in 4% paraformaldehyde in phosphate-buffered saline, incubated overnight at 4°C, and embedded in paraffin. Sections (4 μm thick) were stained with periodic acid–Schiff (PAS) and picrosirius red (PSR). Glomerular area was measured by tracing the outline of the glomerular tuft of at least 50 glomeruli in the cortical fields of PAS-stained specimens. Fibrotic areas were measured digitally on the PSR-stained specimens using a fluorescence microscope (BZ-X800; Keyence, Osaka, Japan). Kidney paraffin sections were also stained with an antibody against phospho-PI3K (P-PI3K) (Ab 182651, Abcam, Cambridge, MA, USA) and phospho-AKT (P-AKT) (Ab 192623, Abcam).

Real-time quantitative reverse transcription polymerase chain reaction analysis

Total RNA was extracted from heart and kidney tissues using ISOGEN (Nippon Gene, Tokyo, Japan). Complementary DNA was synthesized using the SuperScript III First-Strand System (Invitrogen, Carlsbad, CA, USA). Real-time quantitative reverse transcription polymerase chain reaction (RT–PCR) analysis was performed using an ABI PRISM 7000 Sequence Detection System by incubating the reverse transcription products with the TaqMan PCR Master Mix and TaqMan probes (Applied Biosystems, Foster City, CA, USA). The TaqMan probes used for PCR were as follows: collagen type I (Col1), Mm00801666_g1; collagen type III (Col3a1), Mm01254476_m1; alpha smooth muscle actin (α -SMA), Mm01546133_m1; transforming growth factor-beta 1 (TGF- β 1), Mm01178820_m1; tumour necrosis factor alpha (TNF- α), Mm00443258_m1; natriuretic peptide type A (Nppa), Mm01255747_g1; natriuretic peptide type B (Nppb), Mm01255770_g1; angiotensinogen (Agt), Mm00599662_m1; and angiotensin II receptor type 1a (AT1aR), Mm01957722_s1. mRNA levels were normalized to those of 18S rRNA.

Western blotting analysis

Protein expression was analysed by western blotting using tissue homogenates, as described previously.²⁶ Briefly, kidney protein extract was prepared from tissues with sodium dodecyl sulfate-containing sample buffer with the complete protease inhibitor cocktail (Roche, Basel, Switzerland) and phosphatase inhibitor (Thermo Fisher Scientific, IL, USA). Proteins were quantified using the RC DC protein assay kit (Bio-Rad, Hercules, CA, USA). Equal amounts of protein extract were separated by 5–20% sodium dodecyl sulfate–polyacrylamide gel electrophoresis (SDS–PAGE) and transferred to a polyvinylidene difluoride membrane using the iBlot Dry Blotting System (Invitrogen, Paisley, UK). The membranes were blocked with 5% skim milk for 1 h at room temperature and probed with specific primary antibodies to PI3K (Ab 191606, Abcam), P-PI3K (Ab 182651, Abcam), AKT (Ab 179463, Abcam), and P-AKT (Ab 192623, Abcam). Horseradish peroxidase-conjugated goat anti-rabbit IgG secondary

antibodies were added for 1 h at room temperature. The Immobilon Forte Western HRP substrate (Merck, Kenilworth, NJ, USA) was used for detection. The images were captured with auto-exposure, and automatically optimized using ChemiDoc Touch (Bio-Rad Laboratories).

RNA sequencing analysis

Library preparation and sequencing

Quality and quantity of extracted RNA were evaluated by Agilent 4150 TapeStation system following the manufacturer's instructions. Each sample was required to have a RNA integrity number (RIN) above 8.0. We prepared cDNA libraries using NEBNext Ultra RNA Library Prep Kit for Illumina (New England Biolabs) and sequenced the libraries on a Novaseq6000 (Illumina). The average read count per sample was 8 821 889 (range 79 968 604 to 112 187 684). On average, 99.06% of these reads were uniquely mapped, resulting in 24 421 transcripts detected for kidney. Transcripts with an adjusted *P* value (false discovery rate) < 0.01 were considered differentially expressed.

Mapping of sequenced reads and transcript quantification

Following GitHub RNA-seq pipeline riboduct (<https://github.com/msfuji/riboduct>), STAR (v2.7.4a) was used to align the sequenced reads against the mouse genome using the UCSCm10 and FeatureCounts (v2.0.0) was used to quantify the transcripts of the aligned reads using the corresponding UCSCm10 gene annotation model.

Differential gene analysis

The count data generated above were then used as an input for differential gene analysis using the EdgeR (EdgeR version 3.40.0 and R version 4.1.0) was used.

Gene ontology and pathway analysis

To understand the functional roles of the differentially expressed genes (DEGs), ReactomePA (v1.36.0) was used to identify cellular pathways and ClusterProfiler (v4.0.5) was used for gene ontology (GO) analysis.

Statistical analysis

Statistical analyses were performed using Prism software version 9 (GraphPad Software, San Diego, CA, USA). All data are expressed as mean \pm standard error. The differences were analysed as follows. Two-way repeated-measures analysis of variance (ANOVA) followed by Tukey's *post hoc* analysis was performed to determine differences over time between groups (Figures 1A, C, and E and 2I). An unpaired *t*-test was used to determine the differences between the two groups (Figures 5F and 6). One-way ANOVA followed by Tukey's *post hoc* analysis was used for other data. Statistical significance was considered for *P* < 0.05.

Results

ARNI and valsartan exhibit superior antihypertensive effects

The baseline body weight (BW) and systolic BP were identical between the control and treatment groups. Although there were no significant differences in BW trends in each group over the study period (Figure 1A), the rate of weight gain was lower in the ANS-vehicle group than in the control group and higher in the ANS-VAL H group than in the ANS-vehicle group (Figure 1B). In the ANS-vehicle group, systolic BP increased over time (Figure 1C). The ANS-ARNI, ANS-VAL M,

and ANS-VAL H groups exhibited superior antihypertensive effects and significantly suppressed the increase in BP in ANS mice. The antihypertensive effects of valsartan were dose dependent (Figure 1C and D). The antihypertensive effect of ARNI was intermediate between that of VAL M and VAL H, however, not statistically different (Figure 1C and D). There was no difference in HR between the groups (Figure 1E). Heart weight/BW ratio was significantly increased in the ANS-vehicle group compared with the control group, but significantly decreased in the ANS-ARNI, ANS-VAL M, and ANS-VAL H groups compared with the ANS-vehicle group (see Supplementary material online, Figure S1A). Kidney weight/BW ratio was increased in all other groups compared with the control group (see Supplementary material online, Figure S1B).

ARNI prevents cardiac fibrosis and inflammation and reduces cardiac dysfunction in mice with ANS

The area of cardiac fibrosis in the ANS-vehicle group was significantly greater than that in the control group, as shown by histological evaluation using PSR staining (Figure 2A and B). The ANS-VAL M and ANS-VAL H groups also showed significantly larger cardiac fibrotic areas than the control group. However, only in the ANS-ARNI group, there was no increase in cardiac fibrosis compared with the control group, and the increase in cardiac fibrotic areas observed in the ANS-vehicle group tended to be suppressed (Figure 2A and B). Fibrosis-related markers Col1, Col3a1, and TGF- β were also significantly improved or trending towards improvement in the ANS-ARNI group compared with the ANS-vehicle group (Figure 2C–E). Gene expression of inflammation- and tissue damage-related markers TNF- α , Nppa [atrial natriuretic peptide (ANP)], and Nppb [brain natriuretic peptide (BNP)] were also elevated in the ANS-vehicle group, with significant improvement or a trend towards improvement in the ANS-ARNI group, while there was little improvement in both valsartan groups (Figure 2F–H). Progressive exacerbation of decreased myocardial contractility was observed in the ANS-vehicle group (Figure 2I). In the ANS-ARNI group, the rate of decline in LVFS from baseline at 4 weeks was significantly lower than that in the ANS-vehicle group, while the ANS-VAL M and ANS-VAL H groups did not show sufficient prevention (Figure 2J).

ARNI treatment inadequately suppressed albuminuria relative to valsartan treatment

Four weeks after treatment, plasma creatinine concentrations and creatinine clearance were not significantly different among the groups (Figure 3A and B). Albuminuria was markedly higher in the ANS-vehicle group than that in the control group (Figure 3C). The ANS-VAL M and ANS-VAL H groups showed significantly lower amounts of albuminuria than the ANS-vehicle group. However, the ANS-ARNI group did not show as much reduction in albuminuria as the ANS-VAL M and ANS-VAL H groups and was not significantly different from the ANS-vehicle group (Figure 3C). Regarding pathological evaluation, the glomerular area was significantly higher in the ANS-vehicle group than in the control group (Figure 3D). Glomerular swelling was more suppressed in the ANS-ARNI group compared with that in the ANS-vehicle group, but the glomerular area in the ANS-ARNI group was significantly larger than that in the control group. The ANS-VAL M and ANS-VAL H groups also showed significantly less glomerular swelling than the ANS-vehicle group; however, there was no difference between the valsartan and control groups (Figure 3D and E).

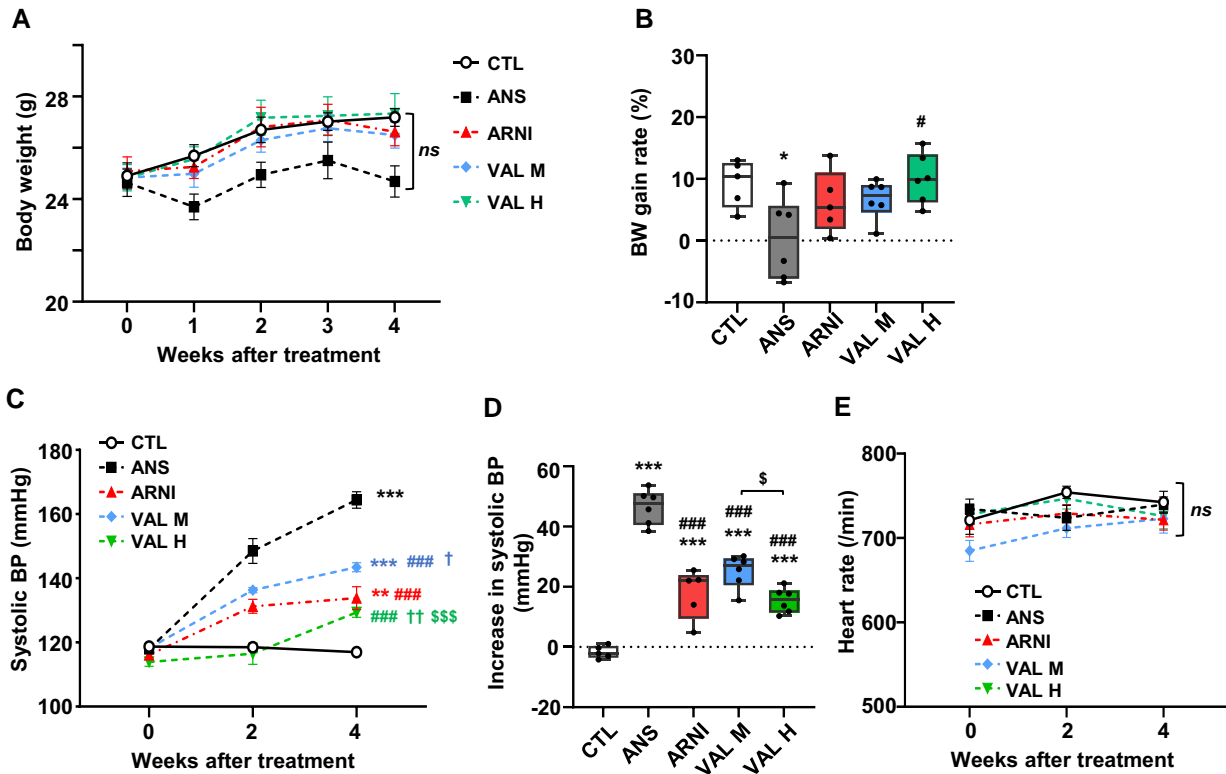


Figure 1 Effects of ARNI and valsartan treatment on BW, BP, and HR in mice with cardiorenal injury. (A) Change in BW, (B) rate of BW gain, (C) change in systolic BP, (D) increase in systolic BP, and (E) change in HR during 4 weeks after treatment in the CTL, ANS-vehicle, ANS-ARNI, ANS-VAL M, and ANS-VAL H groups. Values are expressed as the mean \pm standard error (five or six mice/group). * $P < 0.05$, ** $P < 0.01$, *** $P < 0.001$ vs. the CTL group; # $P < 0.05$, ### $P < 0.001$ vs. the ANS-vehicle group; † $P < 0.05$, †† $P < 0.01$ vs. the ANS-ARNI group; § $P < 0.05$, §§§ $P < 0.001$ vs. the ANS-VAL M group. CTL, control; ANS, angiotensin II infusion, nephrectomy, and salt loading; ARNI, angiotensin receptor-neprilysin inhibitor; VAL M, moderate dose of valsartan; VAL H, high dose of valsartan; BW, body weight; BP, blood pressure; HR, heart rate.

ARNI treatment has insufficient protective effect against kidney fibrosis in mice with ANS

Quantitative evaluation of kidney fibrosis showed that the area of kidney fibrosis in the ANS-vehicle group was significantly larger than that in the control group. Kidney fibrosis was not suppressed in the ANS-ARNI group compared with that in the ANS-vehicle group, while suppression was observed in ANS-VAL M and ANS-VAL H groups (Figure 4A and B). The gene expression of kidney fibrosis-related markers Col1, Col3a1, and α -SMA was significantly higher in the ANS-vehicle group than in the control group (Figure 4C–E). In the ANS-VAL M and ANS-VAL H groups, fibrosis-related gene expression was suppressed compared with that in the ANS-vehicle group, whereas the ANS-ARNI group did not show suppressed expression (Figure 4C–E). Angiotensinogen gene expression in the kidneys was higher in the ANS-vehicle group than in the control group. However, the ANS-ARNI, ANS-VAL M, and ANS-VAL H groups showed a suppression of the increase in angiotensinogen levels observed in the ANS-vehicle group (Figure 4F). There was no difference in AT1aR expression between the groups (Figure 4G). Plasma aldosterone levels were significantly increased in ANS-vehicle group compared with the control group. In contrast, they were not significantly increased in the ANS-ARNI, ANS-VAL M, and ANS-VAL H groups compared with the control (Figure 4H). These findings suggest that the

intra-kidney RAS was suppressed to the same extent in the ANS-ARNI and valsartan groups and that differences in plasma aldosterone levels had little effect on the differential treatment effects of ARNI and valsartan on the kidney.

Renal transcriptomic analysis revealed greater enhancement of molecular

We performed RNA sequencing analysis of kidney tissue to investigate the causes of the differences in kidney phenotypes between ARNI- and valsartan-treated mice with ANS. First, genes that were up-regulated in the ANS-vehicle group relative to the control group were identified. Second, genes that were down-regulated in the ANS-ARNI and ANS-VAL M groups relative to the ANS-vehicle group were identified (Figure 5A). Differentially expressed genes were identified using strict filtering characteristics, with a false discovery rate of $P < 0.01$. Among the genes that were increased in the ANS-vehicle group, we focused on those that were decreased only in the ANS-VAL M group and not in the ANS-ARNI group. This group of genes was chosen because they are considered to be involved in the differences in kidney phenotypes (Figure 5B). Gene ontology enrichment analysis of biological processes and Kyoto Encyclopedia of Genes and Genomes (KEGG) pathway analyses of these differentially expressed 288 transcripts revealed relative enhancement of several molecular signals, such as advanced glycation end product (AGE)—receptors for AGE (RAGE) signalling pathway

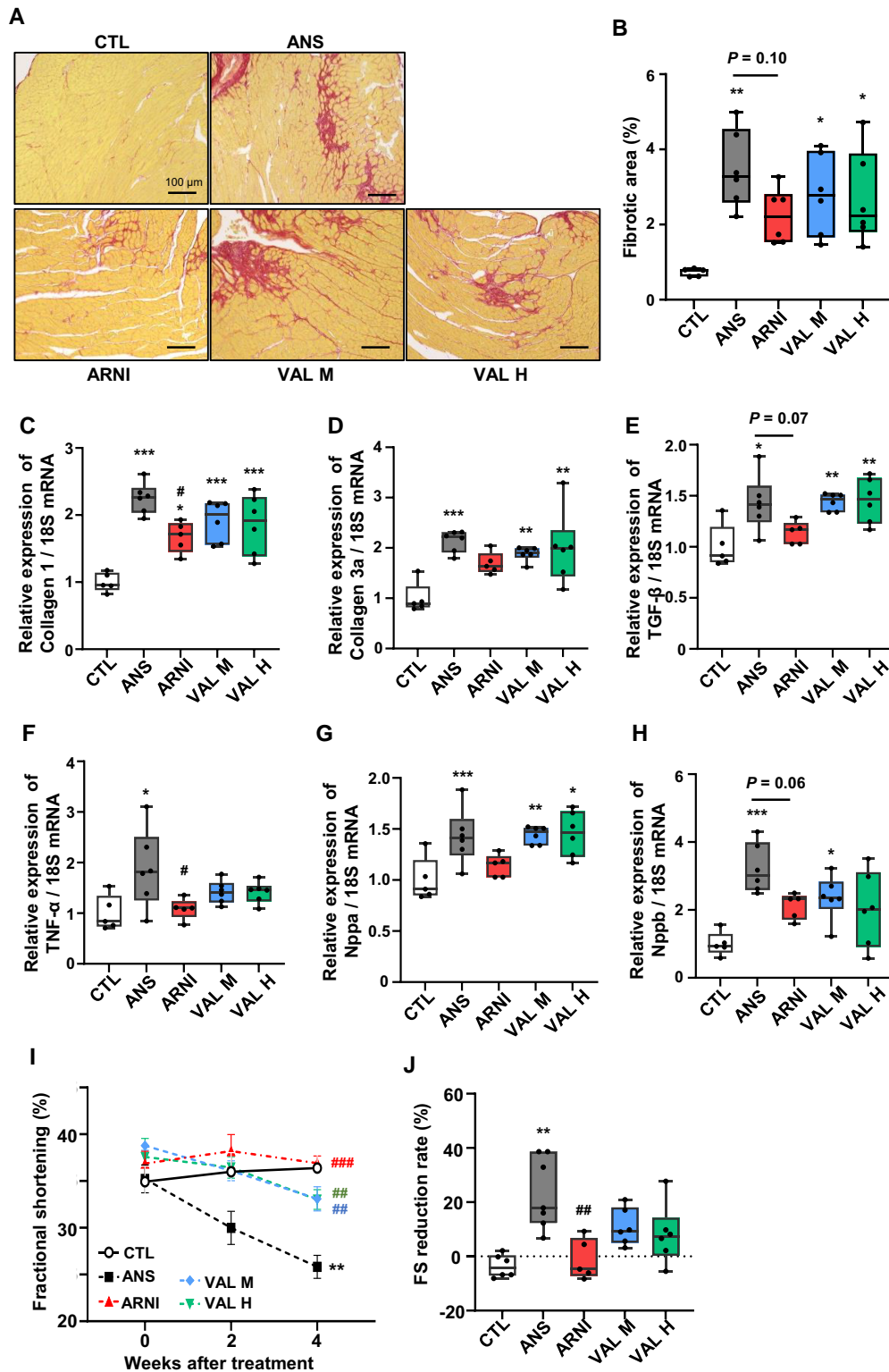


Figure 2 Effects of an ARNI and valsartan treatment on cardiac fibrosis and function in mice with cardiorenal injury. (A) Representative images of the heart stained with picrosirius red (bars = 100 μ m). (B) Quantitative analysis of the fibrotic area in the heart. (C–H) Relative mRNA expression of Col1, Col3a, TGF- β , TNF- α , Nppa, and Nppb in the heart. (I) Cardiac function over 4 weeks and (J) change in rate of cardiac function from baseline to 4 weeks. Values are expressed as the mean \pm standard error (five or six mice/group). * $P < 0.05$, ** $P < 0.01$, *** $P < 0.001$ vs. the CTL group; # $P < 0.05$, ## $P < 0.01$, ### $P < 0.001$ vs. the ANS-vehicle group. CTL, control; ANS, angiotensin II infusion, nephrectomy, and salt loading; ARNI, angiotensin receptor-neprilysin inhibitor; VAL M, moderate dose of valsartan; VAL H, high dose of valsartan; FS, fractional shortening.

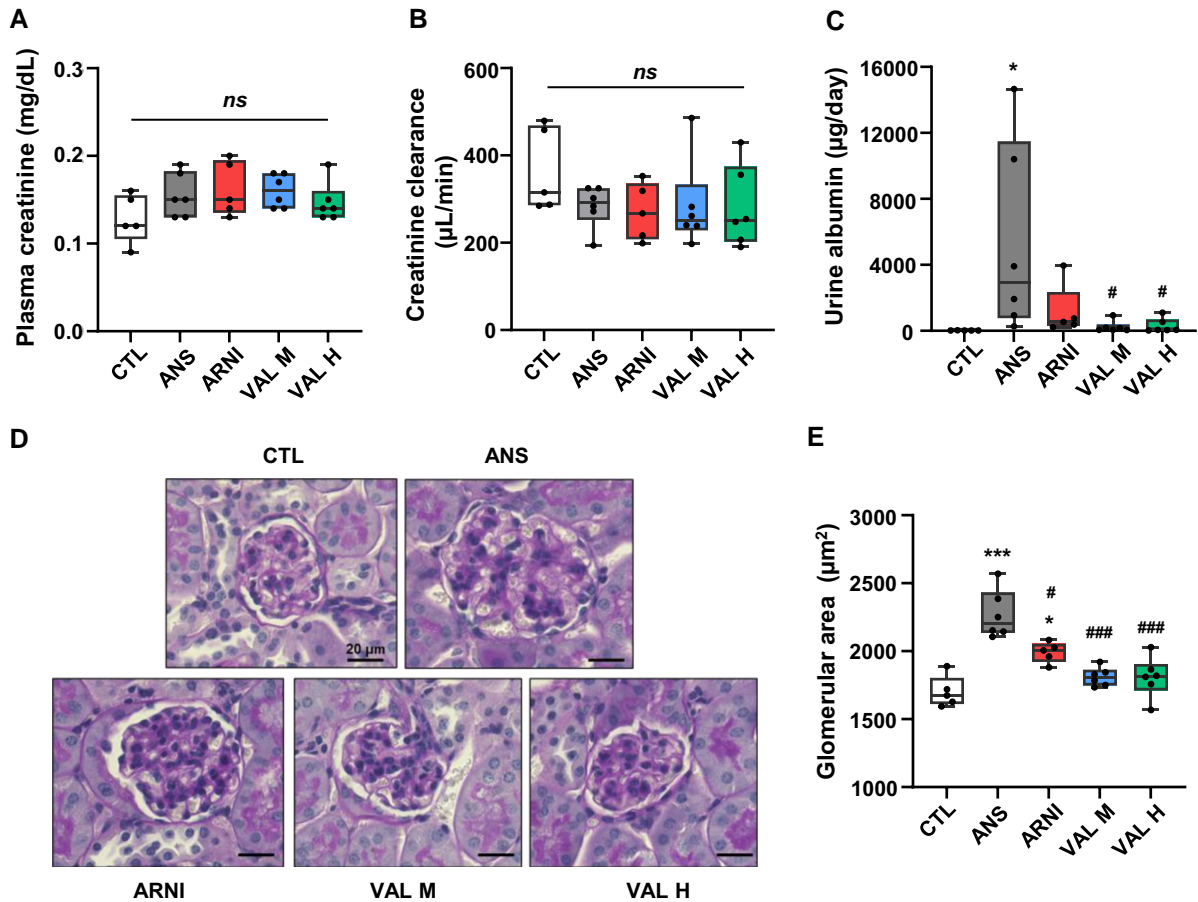


Figure 3 Effects of ARNI and valsartan treatment on kidney function and glomerular size in mice with cardiorenal injury. Kidney function as determined by (A) plasma creatinine concentration, (B) creatinine clearance, and (C) urine albumin. (D) Representative images of kidneys stained with PAS (bars = 20 μm) and (E) quantitative analysis of the glomerular area. Values are expressed as the mean \pm standard error (five or six mice per group). * $P < 0.05$, *** $P < 0.001$ vs. the CTL group, # $P < 0.05$, ### $P < 0.001$ vs. the ANS-vehicle group. CTL, control; ANS, angiotensin II infusion, nephrectomy, and salt loading; ARNI, angiotensin receptor-neprilysin inhibitor; VAL M, moderate dose of valsartan; VAL H, high dose of valsartan; PAS, periodic acid–Schiff.

or PI3K-AKT signalling pathway, along with a group of genes involved in extracellular matrix and collagen metabolism in the kidneys of ARNI-treated ANS mice compared with valsartan-treated ANS mice (Figure 5C and D). Histological findings in the kidneys revealed an enhancement of p-PI3K and p-AKT protein expression in tubular cells in the ANS-ARNI group compared with the ANS-VAL M group (Figure 5E). Western blotting analysis also showed that the P-PI3K/PI3K ratio and P-AKT/AKT ratio were enhanced in the ANS-ARNI group compared with the ANS-VAL M group (Figure 5F).

PI3K inhibitor treatment abolished the differences between the kidney phenotype in ARNI- and valsartan-treated mice with ANS

Kidney transcriptomic analysis and histological findings showed that the relative enhancement of the AGE-RAGE and PI3K-AKT signalling pathways may be involved in the phenotypic differences between the ARNI and VAL M groups. We focused on the PI3K-AKT signalling pathway because it is known to play an important role in the AGE-RAGE

signalling pathway,^{29,30} and its enhancement has been reported to be involved in kidney fibrosis.^{31–33} We hypothesized that inhibiting the PI3K-AKT pathway could reduce the difference in kidney phenotype between ARNI and valsartan treatment in mice with ANS.

Ly294002, a PI3K inhibitor,^{33–35} was injected intraperitoneally at a dose of 30 mg/kg for 3 days per week over 4 weeks after surgery in the ANS-ARNI and ANS-VAL M groups. At 4 weeks after treatment, there was no difference in plasma creatinine concentrations or urine albumin excretion between the ANS-ARNI + Ly294002 and ANS-VAL M + Ly294002 groups (Figure 6A and B). The glomerular area was slightly larger in the ANS-ARNI + Ly294002 group than in the ANS-VAL M + Ly294002 group, but the difference was not statistically significant (Figure 6C and D). The P-AKT/AKT ratio in the kidney in the ANS-ARNI was decreased after PI3K inhibitor treatment (see Supplementary material online, Figure S2). Histological evaluation showed no difference in the fibrotic area between the two groups (Figure 6C and E). There was also no difference in kidney fibrosis-related gene expression between the two groups (Figure 6F and G). In contrast, the cardiac fibrotic area was smaller in the ANS-ARNI + Ly294002 group than in the ANS-VAL M + Ly294002 group (Figure 6H and I). Similarly, the expression of cardiac fibrosis-related genes was lower

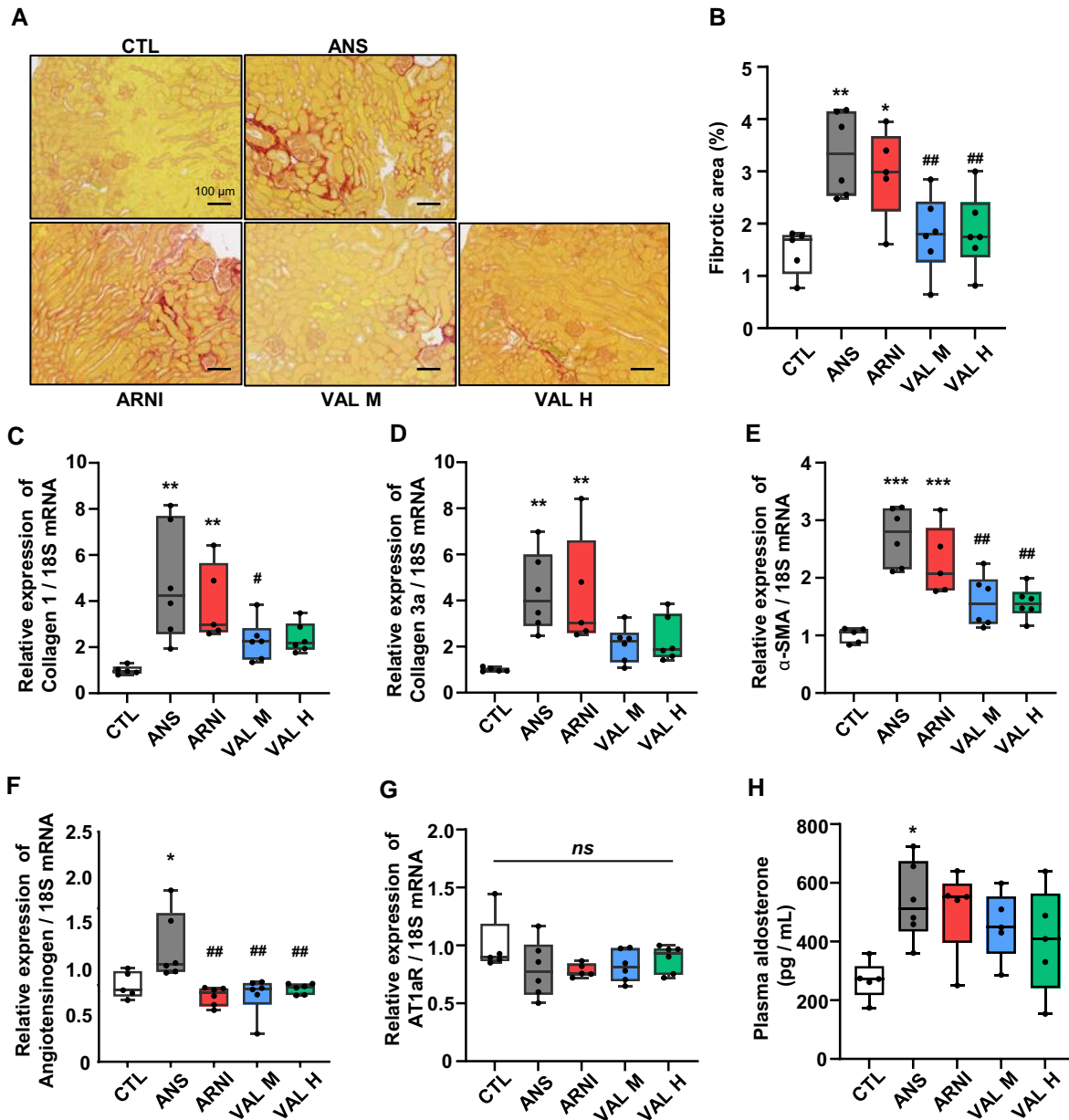


Figure 4 Effects of ARNI and valsartan treatment on kidney fibrosis in mice with cardiorenal injury. (A) Representative images of kidneys stained with picrosirius red (bars = 100 μ m). (B) Quantitative analysis of the fibrotic area in the kidneys. (C–G) Relative mRNA expression of Col1, Col3a, α -SMA, angiotensinogen, and AT1aR in the kidneys. (H) Plasma aldosterone levels in each group. Values are expressed as the mean \pm standard error (five or six mice/group). * P < 0.05, ** P < 0.01, *** P < 0.001 vs. the CTL group; # P < 0.05, ## P < 0.01 vs. the ANS-vehicle group. CTL, control; ANS, angiotensin II infusion, nephrectomy, and salt loading; ARNI, angiotensin receptor-neprilysin inhibitor; VAL M, moderate dose of valsartan; VAL H, high dose of valsartan; SMA, smooth muscle actin; AT1aR, angiotensin II receptor, type 1a.

in the ANS-ARNI + Ly294002 group than that in the ANS-VAL M + Ly294002 group (Figure 6J–L).

Discussion

We investigated the effects of ARNI and valsartan on the heart and kidneys of mice with ANS. Previous reports have indicated that ANS mice are classified as type 3 or 4 CRS because renal damage precedes cardiac

damage.^{25,36,37} In this study, ANS mice was associated with cardiac fibrosis, cardiac dysfunction, overt albuminuria, and kidney interstitial fibrosis. ARNI treatment prevented the increase in cardiac fibrosis and inflammation in mice with ANS, whereas valsartan did not. Additionally, ARNI treatment improved the decline in cardiac function more effectively than valsartan treatment, and these effects were observed independently of the antihypertensive effect. In contrast, ARNI treatment did not ameliorate kidney injury in mice with ANS as effectively as valsartan treatment. Valsartan treatment resulted in

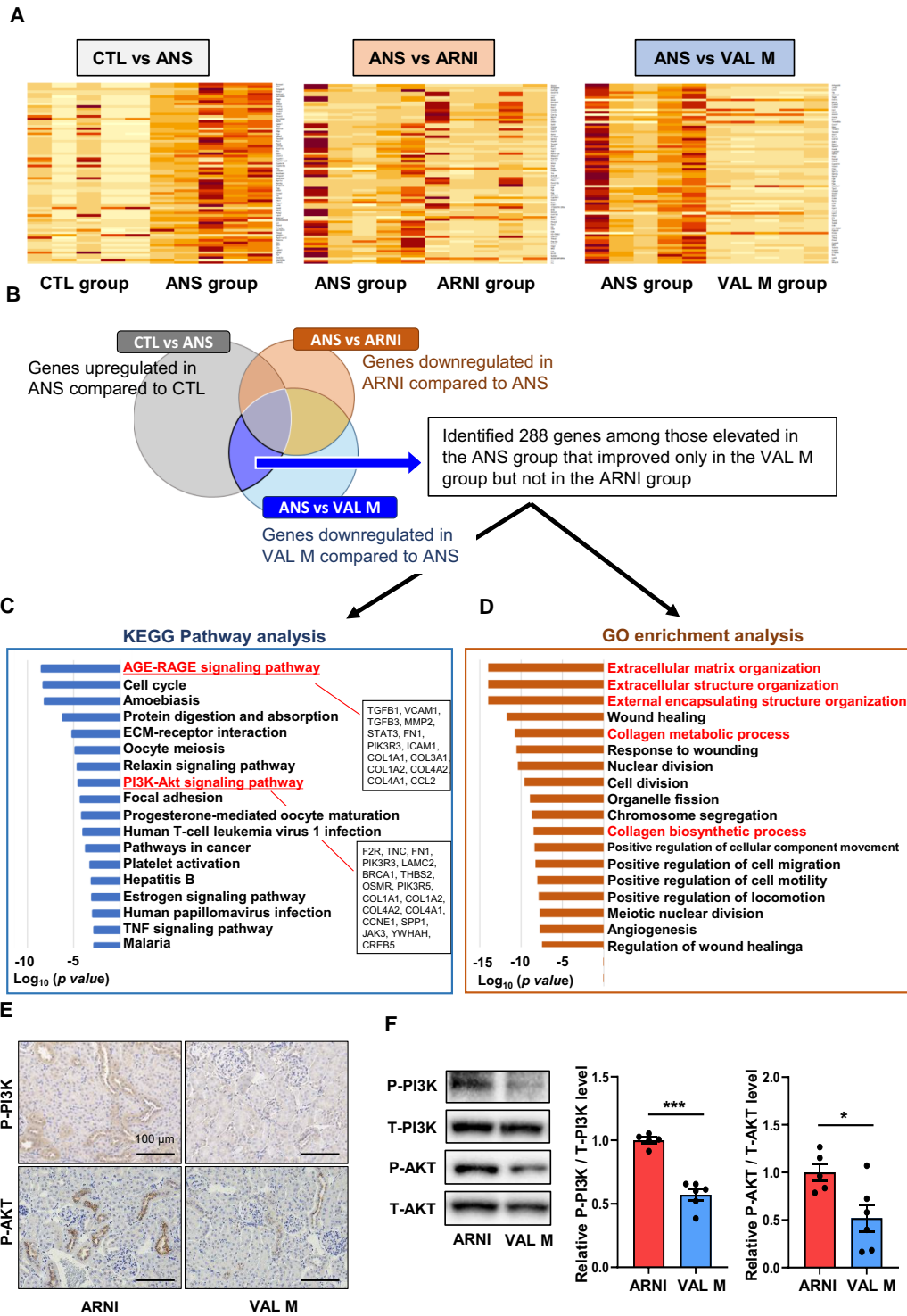


Figure 5 Molecular association of ARNI and valsartan treatment in mice with cardiorenal injury via kidney transcriptomic analysis. (A) Heatmaps of DEGs in CTL, ANS-vehicle, ANS-ARNI, and ANS-VAL M groups. (B) Intersection of genes between up-regulated genes in CTL vs. ANS-vehicle groups and down-regulated genes in ANS-vehicle vs. ANS-ARNI or ANS-vehicle vs. ANS-VAL M groups. (C) KEGG pathway and (D) GO analysis of genes and DEGs that showed improvement only in the ANS-VAL M group. (E) Representative images of kidneys stained with P-PI3K and P-AKT (bars = 100 μm). (F) Kidney P-PI3K/PI3K and P-AKT/AKT protein expression ratio in ANS-ARNI and ANS-VAL M groups by western blotting analysis. CTL, control; ANS, angiotensin II infusion, nephrectomy, and salt loading; ARNI, angiotensin receptor-neprilysin inhibitor; VAL M, moderate dose of valsartan; DEGs, differentially expressed genes; KEGG, Kyoto Encyclopedia of Genes and Genomes; GO, gene ontology; P-PI3K, phospho-phosphoinositide 3-kinase; P-AKT, phospho-AKT.

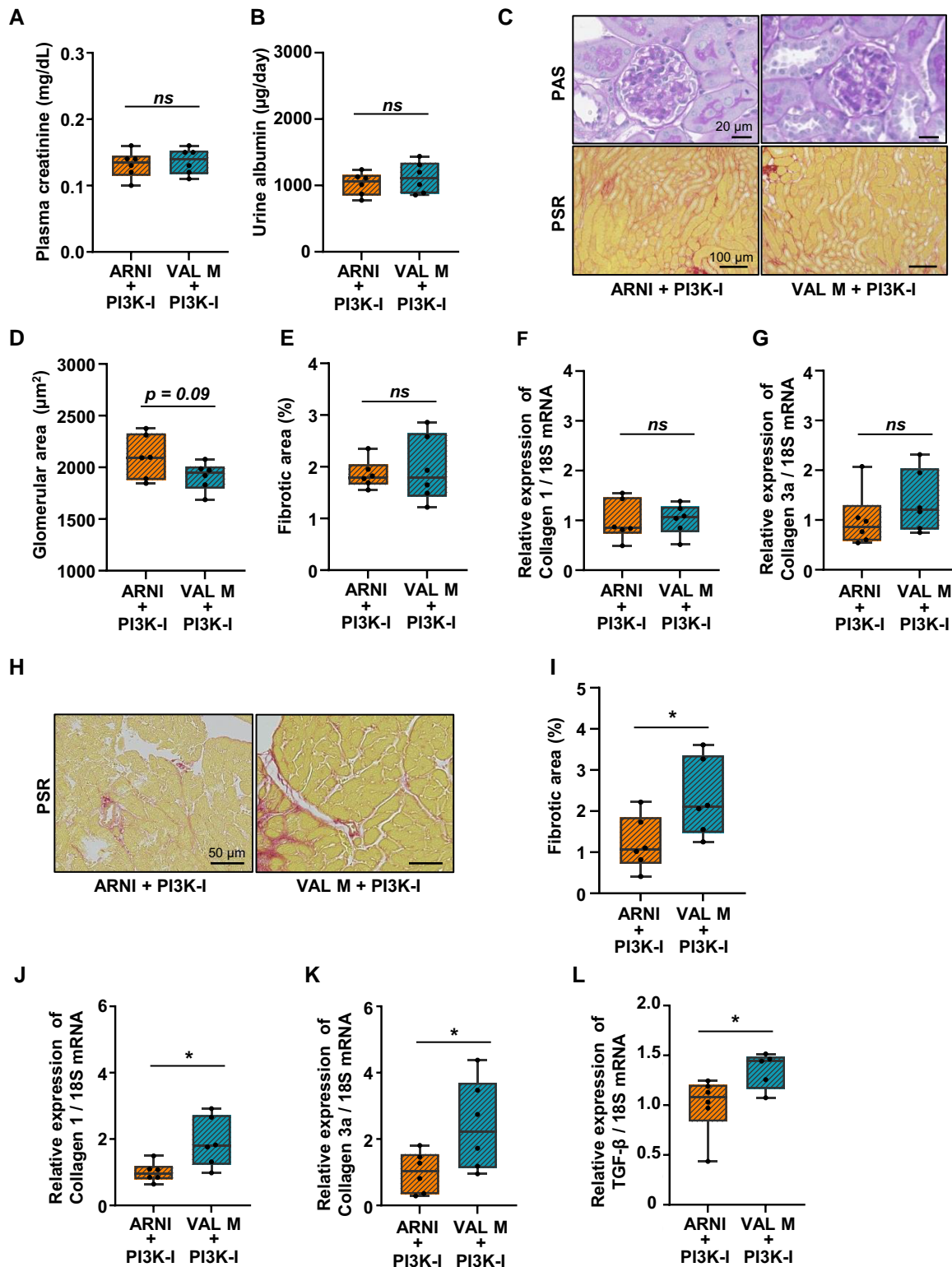


Figure 6 Effects of supplemental PI3K inhibitor treatment with ARNI and valsartan treatment on heart and kidneys in mice with cardiorenal injury. Kidney function was determined by (A) plasma creatinine and (B) urine albumin concentrations. (C) Representative images of kidneys (upper panel, stained with PAS, bars = 20 μm ; lower panel, stained with PSR, bars = 100 μm). Quantitative analysis of (D) glomerular and (E) fibrotic areas. (F, G) Relative mRNA expression of Col1 and Col3a in kidneys. (H) Representative images of the hearts stained with PSR (bars = 50 μm). (I) Quantitative analysis of cardiac fibrotic area. (J–L) Relative mRNA expression of Col1, Col3a, and TGF- β in the heart. Values are expressed as the mean \pm standard error (six mice per group). $*$ $P < 0.05$, vs. the ANS-ARNI + Ly294002 group. VAL M, moderate dose of valsartan; PI3K, phosphoinositide 3-kinase; PAS, periodic acid–Schiff; PSR, picrosirius red.

better attenuation of albuminuria, glomerular hypertrophy, and kidney fibrosis than ARNI treatment. The results of kidney transcriptome analysis revealed that the PI3K-AKT signalling pathway was enhanced in the kidneys of the ANS-ARNI group compared with that in the valsartan group. In addition, the addition of Ly294002, a PI3K inhibitor, to ARNI treatment reduced kidney fibrosis and resolved the phenotypic differences between groups treated with ARNI and valsartan.

Our results demonstrated that the cardioprotective effect of ARNI does not depend on its antihypertensive effect. In patients with HF who are at high risk for cardiovascular disease, BP has a strong positive relationship with the risk of cardiovascular disease,^{38,39} and strict antihypertensive regimens have been reported to contribute to cardioprotective effects.^{40,41} ARNI has a more potent antihypertensive effect than ARBs,^{15,16} and its cardioprotective effect independent of antihypertension in clinical trials remains unclear in some area. The results of this study support the cardioprotective effects of ARNI independent of antihypertension.

In the kidneys, valsartan alone showed more beneficial effects than ARNI in CRS with overt albuminuria. A possible reason for this finding could be the difference in haemodynamic effects of ARNI and valsartan on the kidneys. RAS-Is cause a decrease in intraglomerular pressure due to the dilation of the efferent artery.^{22,42} In contrast, NEP-I contained in ARNIs increases kidney blood flow by enhancing NP activity, leading to increased intraglomerular pressure via predominant afferent artery dilation,^{21,22} increased GFR via mesangial cell relaxation, and an increased filtration coefficient.²¹ Increased intraglomerular pressure and albuminuria cause interstitial damage in addition to direct glomerular damage to the kidneys.⁴³ In the present study, the ARNI group showed higher albuminuria and glomerular hypertrophy than that observed in the valsartan group. These effects may have contributed to the exacerbation of kidney interstitial fibrosis in the ARNI group.

In this study, kidney transcriptomic analysis showed that several molecular signalling pathways in mice with ANS were relatively enhanced by ARNI treatment compared with valsartan treatment, including the PI3K-AKT pathway. The PI3K-AKT pathway is associated with kidney fibrosis.^{31–33} Rodríguez-Peña *et al.*³³ reported that inhibiting the PI3K-AKT pathway suppressed fibrosis in mice with unilateral ureteral obstruction. Furthermore, PI3K-AKT pathway activation is involved in kidney fibrosis in diabetic nephropathy and 5/6 nephrectomy models.^{44,45} The PI3K-AKT pathway is triggered by several signals, such as TGF- β ,³¹ which induce kidney fibrosis via downstream phosphorylation of AKT and activation of the mammalian target of rapamycin.³¹ In the present study, simultaneous add-on treatment with the PI3K-AKT pathway inhibitor to ARNI treatment ameliorated kidney injury, including albuminuria and fibrosis, to levels comparable to those observed in the valsartan treatment group. At the same time, the results showed that the enhancement of the PI3K pathway in the ARNI group was involved in renal fibrosis in the ARNI group. Studies have also reported that the AGE-RAGE pathway is mutually active with the PI3K pathway.^{29,30} In a previous report, proteomic analysis showed that RAGE was up-regulated 14-fold in the kidneys of a rat model of CRS compared with that in controls.⁴⁶ This finding suggests that the AGE-RAGE pathway plays an important role in kidney phenotyping in CRS. In the present study, the AGE-RAGE signalling pathway was also included among the top differential effects of the ARNI and valsartan groups on the kidneys. Therefore, molecular signalling pathways, such as the AGE-RAGE pathway, may also have affected the kidney phenotype of ARNI through the PI3K pathway.

The strength of this study is that by aligning the antihypertensive effects of ARNI and valsartan, we demonstrated the impacts of ARNI and valsartan on the heart and kidney independent of their antihypertensive effects. In addition, we clarified the molecular mechanisms of ARNI in the kidneys of the mice with ANS. For the first time, our kidney transcriptomic analysis revealed that treatment with ARNI may not only cause albuminuria but may also be a risk factor for renal fibrosis due

to its effects on the PI3K pathway. Furthermore, a combined treatment of ARNI and a PI3K inhibitor showed better cardiorenal protection in this model, overcoming the disadvantages of ARNI treatment alone in the kidneys.

This study also had several limitations. First, our animal model did not perfectly replicate actual cardiorenal disease in humans. In addition, there are no human studies to confirm these preliminary results. Future translational studies are needed to investigate the enhancement of the PI3K pathway in humans treated with ARNI. Second, we did not directly evaluate the renal haemodynamic and glomerular effects of ARNI and valsartan. Third, we did not investigate the detailed mechanism underlying the organ-protective effects of ARNI on the heart. Fourth, BP was not assessed using telemetry methods. Fifth, the number of mice per group was relatively small. Moreover, the results of this study were limited to mice with ANS showing high albuminuria and increased kidney hyperfiltration; whether the same results would be obtained under conditions of kidney hypoperfusion or lower albuminuria is unclear. Further research is required to compare the results of multiple disease states and verify the protective effects of the treatments analysed in this study.

In conclusion, in an ANS mouse model of CRS with overt albuminuria, ARNI showed superior cardioprotective effects to those of valsartan independent of their antihypertension effects, while its renoprotective effect was less effective than that of valsartan alone. Subsequent kidney transcriptomic analysis revealed that the PI3K-AKT pathway was significantly activated by ARNI treatment compared with valsartan. Joint treatment with a PI3K-AKT pathway inhibitor and ARNI ameliorated kidney injury, including albuminuria and fibrosis, to levels comparable to those achieved by valsartan. Therefore, supplementing ARNI treatment with a PI3K inhibitor may overcome its negative impact on the kidneys and provide a new treatment option for CRS with massive albuminuria.

Lead author biography



Shunichiro Tsukamoto graduated from Yokohama City University School of Medicine, Japan, with a degree in medicine in 2015, and underwent initial training at Yokohama City Municipal Hospital. Subsequently, he joined the Department of Medical Science and Cardiorenal Medicine, Yokohama City University Graduate School of Medicine, Yokohama, Japan, and is currently a doctoral candidate. His primary research focuses on the fields of kidney diseases, hypertension, diabetes, and obesity.

Data availability

Data from this work will be shared upon reasonable request to the corresponding author. Accession number of RNA-seq data is DRA015661 (DRA in DDBJ).

Supplementary material

Supplementary material is available at *European Heart Journal Open* online.

Authors' contribution

Research conception and study design: SHU.T., H.W., and K.A.; data acquisition: SHU.T., T.U., and Y.S.; data analysis/interpretation: SHU.T.,

T.U., S.U., and SHO.T.; statistical analysis: SHU.T., H.W., and K.A.; writing of the manuscript: SHU.T., H.W., T.U., K.A., S.U., T.S., E.A., SHO.T., SHI.T., K.H., T.Y., S.K., A.Y., and K.T.; supervision or mentorship: H.W., K.A., and K.T. All authors contributed important intellectual content during the drafting and revision of the manuscript. They agree to be personally accountable for their contributions and to ensure that questions about the accuracy or integrity of any portion of the work (even if they were not directly involved) were appropriately investigated and resolved, with documentation if appropriate.

Acknowledgements

We would like to thank A. Kuwae (Yokohama City University), E. Maeda (Yokohama City University), and K. Aoyagi (Yokohama City University) for their help with the experiments. We would like to thank Editage (www.editage.com) for English language editing. Graphical abstract was created with BioRender.com.

Funding

This work was supported by grants from the Yokohama Foundation for Advanced Medical Science, Uehara Memorial Foundation, Japan Society for the Promotion of Science, Japanese Association of Dialysis Physicians.

Conflict of interest: None declared.

References

- Banerjee D, Rosano G, Herzog CA. Management of heart failure patient with CKD. *Clin J Am Soc Nephrol* 2021;**16**:1131–1139.
- Iwama K, Nakanishi K, Daimon M, Yoshida Y, Sawada N, Hirose K, Yamamoto Y, Ishiwata J, Hirokawa M, Kaneko H, Nakao T, Mizuno Y, Morita H, Di Tullio MR, Homma S, Komuro I. Chronic kidney disease and subclinical abnormalities of left heart mechanics in the community. *Eur Heart J Open* 2021;**1**:oeab037.
- House AA, Wanner C, Sarnak MJ, Piña IL, McIntyre CW, Komenda P, Kasiske BL, Deswal A, deFilippi CR, Cleland JGF, Anker SD, Herzog CA, Cheung M, Wheeler DC, Winkelmayer WC, McCullough PA; Conference Participants. Heart failure in chronic kidney disease: conclusions from a Kidney Disease: Improving Global Outcomes (KDIGO) Controversies Conference. *Kidney Int* 2019;**95**:1304–1317.
- Writing Committee; Maddox TM, Januzzi JL Jr., Allen LA, Brethett K, Butler J, Davis LL, Fonarow GC, Ibrahim NE, Lindenfeld J, Masoudi FA, Motiwala SR, Oliveros E, Patterson JH, Walsh MN, Wasserman A, Yancy CW, Youmans QR. 2021 update to the 2017 ACC expert consensus decision pathway for optimization of heart failure treatment: answers to 10 pivotal issues about heart failure with reduced ejection fraction: a report of the American College of Cardiology solution set oversight committee. *J Am Coll Cardiol*. 2021;**77**:772–810.
- Zhang X, Zhou Y, Ma R. Potential effects and application prospect of angiotensin receptor-neprilysin inhibitor in diabetic kidney disease. *J Diabetes Complications* 2022;**36**:108056.
- Nakagawa Y, Nishikimi T, Kuwahara K. Atrial and brain natriuretic peptides: hormones secreted from the heart. *Peptides* 2019;**111**:18–25.
- Sangaralingham S J, Kuhn M, Cannone V, Chen HH, Burnett JC. Natriuretic peptide pathways in heart failure—further therapeutic possibilities. *Cardiovasc Res* 2023;**118**:3416–3433.
- Wu M, Guo Y, Wu Y, Xu K, Lin L. Protective effects of sacubitril/valsartan on cardiac fibrosis and function in rats with experimental myocardial infarction involves inhibition of collagen synthesis by myocardial fibroblasts through downregulating TGF- β 1/Smads pathway. *Front Pharmacol* 2021;**12**:696472.
- Ai J, Shuai Z, Tang K, Li Z, Zou L, Liu M. Sacubitril/valsartan alleviates myocardial fibrosis in diabetic cardiomyopathy rats. *Hellenic J Cardiol* 2021;**62**:389–391.
- Suematsu Y, Miura S, Goto M, Matsuo Y, Arimura T, Kuwano T, Imaizumi S, Iwata A, Yahiro E, Saku K. LCZ696, an angiotensin receptor-neprilysin inhibitor, improves cardiac function with the attenuation of fibrosis in heart failure with reduced ejection fraction in streptozotocin-induced diabetic mice. *Eur J Heart Fail* 2016;**18**:386–393.
- Malek V, Gaikwad AB. Telmisartan and thiorphan combination treatment attenuates fibrosis and apoptosis in preventing diabetic cardiomyopathy. *Cardiovasc Res* 2019;**115**:373–384.
- Liu J, Zheng X, Zhang C, Zhang C, Bu P. Lcz696 alleviates myocardial fibrosis after myocardial infarction through the sFRP-1/Wnt/ β -catenin signaling pathway. *Front Pharmacol* 2021;**12**:724147.
- Ge Q, Zhao L, Ren XM, Ye P, Hu ZY. LCZ696, an angiotensin receptor-neprilysin inhibitor, ameliorates diabetic cardiomyopathy by inhibiting inflammation, oxidative stress and apoptosis. *Exp Biol Med (Maywood)*. 2019;**244**:1028–1039.
- Suematsu Y, Jing W, Nunes A, Kashyap ML, Khazaeli M, Vaziri ND, Moradi H. LCZ696 (sacubitril/valsartan), an angiotensin-receptor neprilysin inhibitor, attenuates cardiac hypertrophy, fibrosis, and vasculopathy in a rat model of chronic kidney disease. *J Card Fail* 2018;**24**:266–275.
- McMurray JJ, Packer M, Desai AS, Gong J, Lefkowitz MP, Rizkala AR, Rouleau JL, Shi VC, Solomon SD, Swedberg K, Zile MR. Angiotensin-neprilysin inhibition versus enalapril in heart failure. *N Engl J Med* 2014;**371**:993–1004.
- Solomon SD, McMurray JJV, Anand IS, Ge J, Lam CSP, Maggioni AP, Martinez F, Packer M, Pfeffer MA, Pieske B, Redfield MM, Rouleau JL, van Veldhuisen DJ, Zannad F, Zile MR, Desai AS, Claggett B, Jhund PS, Boytsov SA, Comin-Colet J, Cleland J, Düngen HD, Goncalvesova E, Katova T, Kerr Saraiva JF, Lelonek M, Merkely B, Senni M, Shah SJ, Zhou J, Rizkala AR, Gong J, Shi VC, Lefkowitz MP. Angiotensin-neprilysin inhibition in heart failure with preserved ejection fraction. *N Engl J Med* 2019;**381**:1609–1620.
- McDonagh TA, Metra M, Adamo M, Gardner RS, Baumhach A, Böhm M, Burri H, Butler J, Čelutkienė J, Chioncel O, Cleland JGF, Coats AJS, Crespo-Leiro MG, Farmakis D, Gilard M, Heymans S, Hoes AW, Jaarsma T, Jankowska EA, Lainscak M, Lam CSP, Lyon AR, McMurray JJV, Mebazaa A, Mindham R, Muneretto C, Francesco Piepoli M, Price S, Rosano GMC, Ruschitzka F, Kathrine Skibellund A; ESC Scientific Document Group. 2021 ESC guidelines for the diagnosis and treatment of acute and chronic heart failure. *Eur Heart J* 2021;**42**:3599–3726.
- Heidenreich PA, Bozkurt B, Aguilar D, Allen LA, Byun JJ, Colvin MM, Deswal A, Drazner MH, Dunlay SM, Evers LR, Fang JC, Fedson SE, Fonarow GC, Hayek SS, Hernandez AF, Khazanie P, Kittleson MM, Lee CS, Link MS, Milano CA, Nwacheta LC, Sandhu AT, Stevenson LW, Vardeny O, Vest AR, Yancy CW. 2022 AHA/ACC/HFSA guideline for the management of heart failure: executive summary: a report of the American College of Cardiology/American Heart Association joint committee on clinical practice guidelines. *Circulation* 2022;**145**:e876–e894.
- Damman K, Gori M, Claggett B, Jhund PS, Senni M, Lefkowitz MP, Prescott MF, Shi VC, Rouleau JL, Swedberg K, Zile MR, Packer M, Desai AS, Solomon SD, McMurray JJV. Renal effects and associated outcomes during angiotensin-neprilysin inhibition in heart failure. *JACC Heart Fail* 2018;**6**:489–498.
- Mc Causland FR, Lefkowitz MP, Claggett B, Anavekar NS, Senni M, Gori M, Jhund PS, McGrath MM, Packer M, Shi V, Van Veldhuisen DJ, Zannad F, Comin-Colet J, Pfeffer MA, McMurray JJV, Solomon SD. Angiotensin-neprilysin inhibition and renal outcomes in heart failure with preserved ejection fraction. *Circulation* 2020;**142**:1236–1245.
- Theilig F, Wu Q. ANP-induced signaling cascade and its implications in renal pathophysiology. *Am J Physiol Renal Physiol* 2015;**308**:F1047–F1055.
- Yamamoto K, Rakugi H. Angiotensin receptor-neprilysin inhibitors: comprehensive review and implications in hypertension treatment. *Hypertens Res* 2021;**44**:1239–1250.
- Tsukamoto S, Uehara T, Azushima K, Wakui H, Tamura K. Updates for cardio-kidney protective effects by angiotensin receptor-neprilysin inhibitor: requirement for additional evidence of kidney protection. *J Am Heart Assoc* 2023;**12**:e029565.
- Haynes R, Judge PK, Staplin N, Herrington WG, Storey BC, Bethel A, Bowman L, Brunskill N, Cockwell P, Hill M, Kalra PA, McMurray JJV, Taal M, Wheeler DC, Landray MJ, Baigent C. Effects of sacubitril/valsartan versus irbesartan in patients with chronic kidney disease. *Circulation* 2018;**138**:1505–1514.
- Noguchi K, Ishida J, Kim JD, Muromachi N, Kako K, Mizukami H, Lu W, Ishimaru T, Kawasaki S, Kaneko S, Usui J, Ohtsu H, Yamagata K, Fukamizu A. Histamine receptor agonist alleviates severe cardiorenal damages by eliciting anti-inflammatory programming. *Proc Natl Acad Sci U S A* 2020;**117**:3150–3156.
- Tsukamoto S, Wakui H, Azushima K, Yamaji T, Urate S, Suzuki T, Abe E, Tanaka S, Taguchi S, Yamada T, Kinguchi S, Kamimura D, Yamashita A, Sano D, Nakano M, Hashimoto T, Tamura K. Tissue-specific expression of the SARS-CoV-2 receptor, angiotensin-converting enzyme 2, in mouse models of chronic kidney disease. *Sci Rep* 2021;**11**:16843.
- Haruhara K, Suzuki T, Wakui H, Azushima K, Kurotaki D, Kawase W, Uneda K, Kobayashi R, Ohki K, Kinguchi S, Yamaji T, Kato I, Ohashi K, Yamashita A, Tamura T, Tsuboi N, Yokoo T, Tamura K. Deficiency of the kidney tubular angiotensin II type1 receptor-associated protein ATRAP exacerbates streptozotocin-induced diabetic glomerular injury via reducing protective macrophage polarization. *Kidney Int* 2022;**101**:912–928.
- Taguchi S, Azushima K, Yamaji T, Urate S, Suzuki T, Abe E, Tanaka S, Tsukamoto S, Kamimura D, Kinguchi S, Yamashita A, Wakui H, Tamura K. Effects of tumor necrosis factor- α inhibition on kidney fibrosis and inflammation in a mouse model of aristolochic acid nephropathy. *Sci Rep* 2021;**11**:23587.
- Sharma I, Tupe RS, Wallner AK, Kanwar YS. Contribution of myo-inositol oxygenase in AGE/RAGE-mediated renal tubulointerstitial injury in the context of diabetic nephropathy. *Am J Physiol Renal Physiol* 2018;**314**:F107–F121.
- Xu D, Kyriakis JM. Phosphatidylinositol 3'-kinase-dependent activation of renal mesangial cell Ki-Ras and ERK by advanced glycation end products. *J Biol Chem* 2003;**278**:39349–39355.
- Zhang YE. Non-Smad pathways in TGF-beta signaling. *Cell Res* 2009;**19**:128–139.
- Hao J, Liu S, Zhao S, Liu Q, Lv X, Chen H, Niu Y, Duan H. PI3K/Akt pathway mediates high glucose-induced lipogenesis and extracellular matrix accumulation in HKC cells through regulation of SREBP-1 and TGF- β 1. *Histochem Cell Biol* 2011;**135**:173–181.

33. Rodríguez-Peña AB, Grande MT, Eleno N, Arévalo M, Guerrero C, Santos E, López-Novoa JM. Activation of Erk1/2 and Akt following unilateral ureteral obstruction. *Kidney Int* 2008;**74**:196–209.
34. Hu S, Hu H, Wang R, He H, Shui H. microRNA-29b prevents renal fibrosis by attenuating renal tubular epithelial cell-mesenchymal transition through targeting the PI3K/AKT pathway. *Int Urol Nephrol* 2021;**53**:1941–1950.
35. Rahmouni K, Haynes WG, Morgan DA, Mark AL. Intracellular mechanisms involved in leptin regulation of sympathetic outflow. *Hypertension* 2003;**41**:763–767.
36. Tharaux PL. Histamine provides an original vista on cardiorenal syndrome. *Proc Natl Acad Sci U S A* 2020;**117**:5550–5552.
37. Muromachi N, Ishida J, Noguchi K, Akiyama T, Maruhashi S, Motomura K, Usui J, Yamagata K, Fukamizu A. Cardiorenal damages in mice at early phase after intervention induced by angiotensin II, nephrectomy, and salt intake. *Exp Anim*. 2023. Online ahead of print.
38. Oparil S, Acelajado MC, Bakris GL, Berlowitz DR, Cifková R, Dominiczak AF, Grassi G, Jordan J, Poulter NR, Rodgers A, Whelton PK. Hypertension. *Nat Rev Dis Primers* 2018;**4**:18014.
39. Won KB, Han D, Choi SY, Chun EJ, Park SH, Han HW, Sung J, Jung HO, Chang HJ. Association between blood pressure classification defined by the 2017 ACC/AHA guidelines and coronary artery calcification progression in an asymptomatic adult population. *Eur Heart J Open* 2021;**1**:oeab009.
40. Pareek M, Vaduganathan M, Byrne C, Mikkelsen AD, Kristensen AMD, Biering-Sørensen T, Kragholm KH, Omar M, Olsen MH, Bhatt DL. Intensive blood pressure control in patients with a history of heart failure: the Systolic Blood Pressure Intervention Trial (SPRINT). *Eur Heart J Cardiovasc Pharmacother* 2022;**8**:E12–e14.
41. SPRINT Research Group; Wright JT Jr, Williamson JD, Whelton PK, Snyder JK, Sink KM, Rocco MV, Reboussin DM, Rahman M, Oparil S, Lewis CE, Kimmel PL, Johnson KC, Goff DC Jr, Fine LJ, Cutler JA, Cushman WC, Cheung AK, Ambrosius WT. A randomized trial of intensive versus standard blood-pressure control. *N Engl J Med*. 2015;**373**:2103–2116.
42. Wenzel RR. Renal protection in hypertensive patients: selection of antihypertensive therapy. *Drugs* 2005;**65**:29–39.
43. Ruggenenti P, Cravedi P, Remuzzi G. Mechanisms and treatment of CKD. *J Am Soc Nephrol* 2012;**23**:1917–1928.
44. Chen J, Wang X, He Q, Bulus N, Fogo AB, Zhang MZ, Harris RC. YAP activation in renal proximal tubule cells drives diabetic renal interstitial fibrogenesis. *Diabetes* 2020;**69**:2446–2457.
45. Zeng R, Yao Y, Han M, Zhao X, Liu XC, Wei J, Luo Y, Zhang J, Zhou J, Wang S, Ma D, Xu G. Biliverdin reductase mediates hypoxia-induced EMT via PI3-kinase and Akt. *J Am Soc Nephrol* 2008;**19**:380–387.
46. Melenovsky V, Cervenka L, Viklicky O, Franekova J, Havlenova T, Behounek M, Chmel M, Petrak J. Kidney response to heart failure: proteomic analysis of cardiorenal syndrome. *Kidney Blood Press Res* 2018;**43**:1437–1450.